

1 **RecDetec – Detecting Recombination and Phylogenetic Information Along Align-**
2 **ments**

3 Heiko A. Schmidt[#], Moritz B. Reinhardt, Tung Lam Nguyen and Arndt von Haeseler

4 Center for Integrative Bioinformatics Vienna (CIBIV), Max F. Perutz Laboratories (MFPL),
5 Vienna, Austria; University of Vienna, Medical University of Vienna, Vienna, Austria

6 Running title: Detecting Recombination and Phylogenetic Information

7 Keywords: recombination detection; phylogenetic information; alignment assessment; over-
8 lapping recombinations; bootscanning

9 #Corresponding author: `heiko.schmidt@univie.ac.at`

10

11 word counts:

12 abstract: 137 words

13 main text: 3520 words

14 **Abstract**

15 Recombination is a common mechanism, occurring with high rates especially in RNA viruses.
16 Thus, phylogeny reconstruction of viruses is challenging and detecting recombinants and re-
17 combination break points has become an important task when analyzing viral genomes. If
18 the data contain several recombinants or, moreover, recombinants originating from overlap-
19 ping recombinations (i.e. independent recombination events that involve parental strains
20 from the same group), recombination detection gets difficult. Here, we utilize the infor-
21 mation obtained from initial ML phylogenetic reconstructions on sliding windows to reveal
22 recombinants and recombination breakpoints. Our approach detects complex recombination
23 patterns without having to recompute the phylogenetic trees. The approach is implemented
24 in the software RecDetec. The software also allows for using parallel computing platforms
25 to reduce runtime. An illustrative example highlights the utility of RecDetec. Finally, our
26 results are compared to other approaches.

27 **Introduction**

28 Determining the history of a viral strain has become a common task in virus research, e.g.
29 in genotyping strains (4, 2) or when reconstructing the migration paths of an epidemic
30 (5, 19, 20). However, variation of evolutionary rates, different selection pressures (either
31 over time or along the genome), reassortment and recombination (14, 10) confound the
32 reconstruction of the history. Especially in viruses recombination is a major force promoting
33 adaptation, e.g., for an effective evasion of the immune or other defense systems of their hosts
34 (10), or for promoting drug resistance (3). Thus, phylogenetic reconstruction for viruses is
35 still a challenging task.

36 In Eukaryotes and DNA viruses recombination usually requires enzyme-mediated double

37 strand breaks (16), whereas in RNA viruses and retroviruses RdRP (RNA-dependent RNA
38 polymerase) and RT (reverse transcriptase) can switch their RNA-template during replica-
39 tion, thus, connecting the information of potentially different parental template sequences
40 (27). Rates as high as 2-3 RNA recombination events per genome and replication have
41 been reported for HIV (11). Although recombination certainly also occurs among identical
42 sequences, for a recombination event to be detectable, the parental strains co-infecting the
43 same cell have to exhibit a certain degree of sequence divergence. If recombination takes
44 place between divergent parents, the different histories of the recombined parts can be inves-
45 tigated by phylogenetic approaches. While the detection of a single recombinant strain in a
46 collection of aligned sequences is not too difficult, this task is hard if the alignment contains
47 several recombinants. The analysis gets even more difficult with overlapping recombinations,
48 that is, recombinants originating from independent recombination events having parents be-
49 longing to the same group of reference strains in overlapping genomic regions.

50 Owing to the importance of recombination methods abound to detect recombination in
51 genomic sequences (e.g., (13, 22)), among them the popular bootscanning (23), a sliding
52 window approach. Bootscan implementations (15, 17, 2) use an alignment as input. The
53 sequences of the alignment are typically assigned to disjoint (reference) groups and for each
54 group the consensus sequence is computed or an arbitrary sequence is selected to represent
55 its group (23). For a putatively recombinant query group bootscanning then searches for
56 possible parents within the reference groups and the corresponding recombination break-
57 points. To that end the alignment is split into overlapping windows and each window is
58 subjected to a bootstrap analysis (8, 7). Finally, the bootstrap support for clustering the
59 query group with each of the reference groups are collected for each window and plotted
60 along the alignment. Under the assumption that the query group will get high bootstrap
61 support if clustered with its parental subtypes in the respective windows, the recombination

62 breakpoints can be detected (cf. Fig. 1). However, if the user redefines query or reference
63 groups or wants to focus on a relevant subset of sequences, one has to redo the complete time
64 consuming analysis. There are two stand-alone implementations (15, 17) of bootscanning for
65 Microsoft Windows. In addition, some web tools employ bootscanning for subtyping query
66 sequences of specific viruses (4, 2).

67 Here, we present RecDetec to study recombination using maximum likelihood (ML) phy-
68 logenies. RecDetec finds simple recombinants and also detects overlapping recombination.
69 Furthermore, the user can redefine reference and query groups or exclude strains without
70 repeating the time consuming phylogenetic inference. Finally, RecDetec also analyzes the
71 phylogenetic information content in the alignment. RecDetec is an exploratory tool that
72 runs on Linux/Unix, MacOSX and Windows.

73 **Materials and Methods**

74 **Recombination analysis with RecDetec**

75 RecDetec takes as input a multiple sequence alignment of genomic sequences to which the
76 sliding-window approach (cf. Fig. 1) is applied, where window size and step size can be
77 specified by the user. RecDetec computes two support values. First it computes boot-
78 strap supports for each window based on maximum likelihood trees inferred with IQPNNI
79 (18) which results in *ML bootscanning* diagrams. Second, RecDetec determines the sup-
80 port values using the Quartet Puzzling (QP) method implemented in the TREE-PUZZLE
81 program (28, 25) to produce *QP-scanning* diagrams. Contrary to the original bootscanning
82 description, where user-defined groups of sequences are represented as consensus sequence or
83 by an arbitrary representative, RecDetec reconstructs trees for all sequences. All splits, i.e.
84 branches, found during the bootstrap analysis are collected and their frequencies are counted

85 for each window. The sequences are usually assigned to user-defined disjoint groups, namely
86 one query group where recombinants are suspected and a set of reference groups containing
87 potential parents. Groups should typically comprise sequences with the same phylogenetic
88 background tracing back to a single common ancestor, but also other user-defined groups
89 can be analyzed. Groups may comprise pure (i.e. not recombined) sequences of the same
90 subtype or taxonomic group, but can also consist of recombinant forms. Each group can
91 contain one or more sequences.

92 Finally, the bootstrap values for query group/reference group clusters are computed. To
93 that end the support values are computed for branches separating the query group se-
94 quences $\{Q_1 \dots Q_l\}$ together with the sequences of exactly one reference group $\{G_1 \dots G_k\}$
95 from the remaining sequences $\{R_1 \dots R_m\}$. The support value for a branch separating
96 $\{Q_1 \dots Q_l, G_1 \dots G_k\}$ from the rest is computed for each query group reference group pair
97 and for each window along the alignment. These values are then plotted along the alignment.
98 In addition, RecDetec offers the possibility to visualize the bootstrap consensus tree for any
99 window employing the FigTree software (<http://tree.bio.ed.ac.uk/software>).

100 RecDetec offers further analyses at no additional computation cost. RecDetec can plot the
101 bootstrap (8, 7) or puzzle support (25, 28) values for each user-defined group and each sliding
102 window. The resulting diagrams visualize the group support as a measure of phylogenetic
103 stability of groups along the alignment. This allows to detect genomic regions where the
104 support of a group is lost or to detect unreasonable groups, if they are not supported at all.

105 **Analyzing subsets of sequences:** In RecDetect the user can exclude interfering recom-
106 binant sequences when generating bootscanning or group support diagrams, if they would
107 otherwise obstruct the signal. In the following we describe how RecDetec obtains the support
108 values for the respective diagrams in this case.

109 For the complete set of sequences, i.e. no sequences excluded, the support for a common

110 subtree of sequences $\{W_1 \dots W_k\}$ (e.g. the query group with one reference group) can be
111 obtained directly from the collection of bootstrap data. This is straightforward, because a
112 split that bipartites all sequences into $\{W_1 \dots W_k\}$ and the remaining sequences $\{R_1 \dots R_m\}$
113 is unique.

114 If one sequence $\{X\}$ is excluded when obtaining the support of the group $\{W_1 \dots W_k\}$
115 against the remaining taxa $\{R_1 \dots R_m\}$, $\{X\}$ can cluster with $\{W_1 \dots W_k\}$ (Fig. 2a) or with
116 the remaining taxa $\{R_1 \dots R_m\}$ (Fig. 2b). In the special case of $\{X\}$ being located between
117 $\{W_1 \dots W_k\}$ and $\{R_1 \dots R_m\}$ (cf. Fig. 2c) both relevant splits exist in the same tree. For
118 visualization we use the split from b_i and b_j that maximizes the support value. Note, that
119 after excluding a sequence $\{X\}$ it is included neither in $\{W_1 \dots W_k\}$ nor in $\{R_1 \dots R_m\}$.

120 When excluding more sequences, say $\{X_1 \dots X_q\}$, the support values of the relevant splits
121 can still be collected by examining splits separating $\{W_1 \dots W_k\}$ from the remaining se-
122 quences $\{R_1 \dots R_m\}$, where each 'excluded' sequence clusters either with $\{W_1 \dots W_k\}$ or
123 $\{R_1 \dots R_m\}$. From all 2^q possible splits of that kind we use for visualization the split with
124 maximal support.

125 **Visualizing phylogenetic information content:** Two means have been implemented to
126 visualize the phylogenetic information content in the windows induced sub-alignment. First,
127 likelihood mapping (29) is used to measure phylogenetic information in each window using
128 the maximum likelihood values for the three trees relating four sequences (quartets). If one
129 tree has a high likelihood compared to the others, the quartet is called a *resolved quartet*. If
130 the likelihood from two trees are more or less the same and larger than the third likelihood,
131 the quartet is a *partly resolved quartet*, otherwise it is an *unresolved quartet*. The percentages
132 of resolved, partly resolved and unresolved quartets are plotted along the alignment. A
133 high percentage of unresolved quartets marks alignment windows with little phylogenetic
134 information (26, 29).

135 Second, the amount of parsimony informative sites (30) can be displayed. We use the
136 following extended definitions of parsimony informative sites: A parsimony *informative site*
137 is an alignment column that contains at least two different nucleotides and at least two of
138 the nucleotides occur at least twice. A parsimony informative site is *partly informative*, if
139 some nucleotides nucleotides occur only once, or if gaps or other ambiguous characters (like
140 N) occur at that site. All other alignment columns are (*parsimony*) *uninformative*. Among
141 these, two types of constant sites are defined. *Completely constants sites* contain only one
142 nucleotide in all sequences, while *constant sites* can contain gaps or ambiguous characters
143 (like N) besides one single nucleotide. The counts for these categories can also be plotted
144 for each window and display the parsimony phylogenetic information content.

145 **Parallel execution of the phylogenetic reconstructions:** To save computation time, RecDe-
146 tec supports execution on parallel computing platforms. For instance, freely available
147 scheduling or middleware software can distribute the tasks of the RecDetec workflow to
148 parallel computing platforms like clusters, grids, cloud computing environments or just local
149 multicore machines (9, 32, 31). After the phylogenetic bootstrap analyses are finished the
150 reconstructed trees can then be imported into RecDetec for the final analysis. However, the
151 reconstructions can just as well be performed inside RecDetec without employing a cluster.

152 Results

153 **An example scenario with overlapping recombination:** We simulate a dataset assuming
154 a scenario of overlapping recombinations, i.e. two independent recombinants have parental
155 strains in the same reference group.

156 To this end, we generate an alignment of 7000bp length and eleven 'genomes' (*A1, A2, B1,*
157 *B2, C1, C2, D1, D2, O1, O2, X*) containing three regions with different evolutionary rates.

158 In the first 500bp of the sequences the evolutionary rates were 50-fold increased, while the
159 last 500bp of the sequences have a 50-fold reduced evolutionary rate with respect to regions
160 501-6500bp. Sequences have been simulated using seq-gen (21) according to the following
161 evolutionary scenario. The dataset comprises a recombinant sequence $\{X\}$ as query group
162 and four reference groups $\{A1, A2\}$, $\{B1, B2\}$, $\{C1, C2\}$, $\{D1, D2\}$ and outgroup $\{O1, O2\}$,
163 where $\{B1, B2\}$ is also recombinant creating the scenario of overlapping recombinations.
164 The evolutionary history of the sequences is depicted in Fig. 3a. The recombination events
165 lead to chimeric sequences for $\{X\}$ and $\{B1, B2\}$. $\{X\}$ shares a common history (Fig. 3b)
166 with $\{C1\}$ in region **a** (1-2000bp) and with $\{A2\}$ otherwise (2001-7000bp), while group
167 $\{B1, B2\}$ shares a common history (Fig. 3c) with $\{A1, A2\}$ in regions **a, b, d** (1-3500bp and
168 5001-7000bp) and with $\{D2\}$ in region **c** (3501-5000bp). The underlying phylogenetic trees
169 for the four regions **a-d** are depicted in Fig. 4a-d.

170 **RecDetec analysis:** Tree reconstructions are performed for ML bootscanning with window
171 size 300, step size 25. For the initial recombination analysis, we assume the sequences are
172 grouped based on some prior knowledge (like, for instance, preliminary phylogenetic analysis
173 of the first 2000bp of the genomes) into the reference groups $\{A1, A2, B1, B2\}$, $\{C1, C2\}$,
174 $\{D1, D2\}$ and $\{O1, O2\}$.

175 Prior to the recombination analysis, we assess the phylogenetic information in the align-
176 ment and visualize the phylogenetic information content based on likelihood mapping (Fig. 4e).
177 The red curve displays the fraction of unresolved quartets. It is high at the ends of the
178 alignment, indicating only very little or no phylogenetic information. Now we can use the
179 parsimony informative sites diagram (Fig. 4f) to determine whether the lack of phylogenetic
180 information is due to small sequence diversity or noise. On the right end of the alignment
181 the number of constant sites is very high implying low diversity, whereas the left end of the
182 alignment has a high number of parsimony informative sites (up to 100%, Fig. 4f). However,

183 since the corresponding fraction of resolved quartets is low in the phylogenetic information
184 plot (Fig. 4e), this indicates that the phylogenetic signal is lost due to the high mutation
185 rate in that part of the alignment. This analysis shows that the first and the last 500bp of
186 the alignment are not suitable for phylogenetic analysis. We will ignore these regions in the
187 following.

188 Next we choose $\{X\}$ as query group for ML bootscanning (Fig. 4g). In region **a** we observe
189 high bootstrap support for the cluster joining $\{X\}$ and $\{C1, C2\}$ (red curve), whereas the
190 support drops to 0 elsewhere. In regions **b** and **d** we observe high support for a cluster of
191 $\{X\}$ with $\{A1, A2, B1, B2\}$ (turquoise curve). No grouping of $\{X\}$ with any reference group
192 is observed in the region **c**. Fig. 4g shows a clear signal for different evolutionary histories
193 before and after position 2000 ($\{X\}$ being related to $\{C1, C2\}$ and to $\{A1, A2, B1, B2\}$).
194 But no statement about the phylogenetic history of $\{X\}$ in region **c** is possible.

195 To further elucidate this, we plot the group support for $\{A1, A2, B1, B2\}$ excluding the
196 recombinant $\{X\}$ (Fig. 4h). The plot reveals that the reference group has no phylogenetic
197 support in region **c**, i.e., a subtree with sequences $\{A1, A2, B1, B2\}$ is not found (bootstrap
198 support close to zero). Bootstrap consensus trees reconstructed for region **c** confirm this.
199 However, in this tree we observe that $\{B1, B2\}$ groups with $\{D1, D2\}$ in region **c**. Thus,
200 $\{B1, B2\}$ is possibly a recombinant strain. To investigate this we plot an ML bootscan
201 diagram with query group $\{A1, A2\}$, excluding the putatively recombinant groups $\{X\}$ and
202 $\{B1, B2\}$ from the analysis (Fig. 4i). This plot shows no signal that region **c** of $\{A1, A2\}$
203 was exchanged by recombination. Then we use $\{B1, B2\}$ as query group and exclude $\{X\}$
204 and $\{A1, A2\}$. Fig. 4j shows that $\{B1, B2\}$ clusters 'correctly' with $\{O1, O2\}$ in regions **a**,
205 **b** and **d** (magenta curve), while it clusters with $\{D1, D2\}$ in region **c** (cyan curve). This
206 supports that $\{B1, B2\}$ is indeed a recombinant form.

207 Since the group $\{A1, A2, B1, B2\}$ contains pure and recombinant sequences, we will re-

208 analyze the putatively recombinant groups $\{X\}$ and $\{B1, B2\}$ with reference groups $\{A1, A2\}$,
209 $\{C1, C2\}$, $\{D1, D2\}$ and $\{O1, O2\}$. One recombinant can obscure the signal of the other
210 (overlapping) recombinant in the diagrams because they share common subtrees with the
211 same parents in some regions. Thus, the two recombinant groups will be analyzed separately,
212 each group will act as a query excluding the other recombinant group when plotting the
213 diagram. Now the bootscan plot (Fig. 4k) for $\{X\}$ (excluding $\{B1, B2\}$) shows nicely the
214 recombination pattern for $\{X\}$ as being a recombinant of $\{C1, C2\}$ (region **a**, red curve)
215 and $\{A1, A2\}$ (regions **b-d**, blue curve). Likewise, Fig. 4l shows that $\{B1, B2\}$ is indeed
216 a recombinant of sequences related to $\{A1, A2\}$ (regions **a, b, d**, blue curve) and $\{D1, D2\}$
217 (region **c**, turquoise curve). Thus, we could show that $\{X\}$ and $\{B1, B2\}$ are indeed overlap-
218 ping recombinants and detected the regions where the different recombination break points
219 are located. Please note, that the time consuming phylogenetic analysis was only run once
220 at the beginning.

221 **Simplot analysis:** In addition, we analyzed this dataset using bootscanning where groups
222 are represented by their consensus sequences as implemented in SimPlot (15) (using the same
223 parameters for window size, step width, and evolutionary model as above). The SimPlot
224 bootscan diagram (Fig. 5) shows the recombination breakpoint at 2000bp and the relation-
225 ship of $\{X\}$ with $\{C1, C2\}$ before and with $\{A1, A2, B1, B2\}$ after the breakpoint. However,
226 there are no hints that $\{A1, A2, B1, B2\}$ contains recombinant sequences.

227 **GARD analysis:** We analyze the dataset with GARD (12), another ML-based recombina-
228 tion detection tool which uses a genetic algorithm to determine recombination break points.
229 GARD identifies breakpoints at about 500bp, 2000bp, 3500bp, 5000bp and 6500bp, marking
230 the boundaries of all six genomic regions from the simulation. However, GARD cannot detect
231 whether the breakpoints were caused by recombination events or by changing evolutionary

232 rates.

233 **Discussion**

234 The bootscanning approach has proven useful in many recombination studies during the past
235 decades. In contrast to previous bootscanning implementations, RecDetec generates support
236 values based on ML approaches. Support values can either be obtained from ML phyloge-
237 nies producing ML bootscanning diagrams or by Quartet Puzzling producing QP-scanning
238 diagrams. While the former performs more rigorous tree searches, the latter typically pro-
239 duces the ML-based QP support values more quickly. ML approaches have the advantage
240 of employing a well-established statistical framework, which is known to produce good re-
241 sults in practice. Although the recombination detection tool GARD (12) could identify the
242 boundaries of all six genomic regions, not all of these are caused by recombination events.
243 RecDetec also found the breakpoints (Fig. 4), but also allows for analysis to find the causes
244 of the different regions.

245 As mentioned, other bootscanning implementations usually reduce sequence groups to one
246 representative or consensus sequence. While this saves running time, consensus can lead to
247 artificial sequences which do not well reflect the features of the represented sequences (6).
248 We show that the signal of wrongly defined groups (e.g., joining pure and recombinant se-
249 quences) can easily get lost in the consensus sequence, leaving no hint (cf. Fig. 5) that the
250 true underlying structure contains overlapping recombinants. Such incompletely recovered
251 histories can easily lead to wrong assumptions about the history of infectious virus strains.
252 Keeping all sequences separate as in RecDetec has the additional advantage that trees can
253 typically be reconstructed more accurately due to the additional information present (24).
254 Separate sequences, on the other hand, can lose support for a joint cluster due to several
255 reasons. The support might be lost because related recombinant sequences cluster in a joint

256 subtree, but also due to lack of phylogenetic signal. With separate sequences, however,
257 RecDetec can assess the phylogenetic stability of the groups along the alignment. If groups
258 are not stable along the alignment closer examination is required, and RecDetec offers means
259 to examine whether the instability of groups in an alignment region was caused by recom-
260 binants or by the regional lack of phylogenetic information. Since it is crucial for bootscan
261 analyses to define groups of sequences comprising related pure sequences or related recombi-
262 nants based on prior knowledge, visualizing the phylogenetic stability of groups is a valuable
263 tool to assess the quality of user-defined groupings. Undetected recombinant groups or sub-
264 types may exist even in well-studied viruses such as HIV, making the assessment of reference
265 groups for recombinants even more important. While HIV-1 subtype G was assumed to be
266 a pure subtype for a long time, it was shown to be a recombinant form (1) and thus possibly
267 confounding the phylogenetic signal of related sequences.

268 In a phylogenetic analysis, known (and yet unknown) recombinants may naturally disturb
269 the subtree support of their parental groups because in different genomic regions they cluster
270 with their respective relatives. To analyze such cases RecDetec allows for excluding (puta-
271 tively recombinant) sequences without having to re-compute the phylogenetic reconstruc-
272 tions. This enables the analysis of recombination or phylogenetic stability in the presence of
273 several recombinants and even overlapping recombinants. By studying recombinant groups
274 separately, excluding the other overlapping recombinants in turn, it is possible to examine
275 their relationships.

276 Plotting phylogenetic information and informative sites diagrams allow for quickly detect-
277 ing genomic regions with very low or high divergence, thus, containing no information or
278 accumulated noise. This, together with the group support plots, is necessary to correctly
279 interpret bootscan results to find out whether the loss of support of relationship is caused by
280 recombination, by effects of data quality or by wrong assumptions about reference groups.

281 The assessment of phylogenetic information along an alignment is certainly an important
282 task prior to many phylogenetic analysis of other (even non-recombinant) datasets.

283 Finally, we point out that RecDetec is an exploratory tool to detect and analyze complex
284 evolutionary patterns. We showed that it was possible to identify and isolate different
285 recombinants by excluding sequences and, thus, to visualize their individual relationships.

286 In summary, RecDetec offers flexible ways to detect (overlapping) recombination events,
287 to assess phylogenetic informativeness of genomic regions prior to the actual phylogenetic
288 reconstruction or to examine the support of a joint subtree of sequences of interest along a
289 given alignment. This would be helpful not only to study viral sequences known to recombine,
290 but also to other phylogenetic analyses not dealing with recombination to detect why and
291 where some subtrees are not well supported in a phylogenetic reconstruction or why some
292 reconstructions do not work at all. RecDetec adds complementary analyses and assessments
293 which were not available by other bootscanning implementations. Furthermore, it makes
294 bootscanning analyses accessible to a wider range of operating systems and makes use of
295 modern maximum likelihood methods for this kind of analysis.

296 **Acknowledgments**

297 The authors would like to thank Martina Kutmon for preparing an early version of the
298 software and for suggesting its name. Financial support by the Austrian Science Fund
299 (FWF, I760) to AvH is gratefully acknowledged.

300 **References**

301 [1] Abecasis AB, Lemey P, Vidal N, de Oliveira T, Peeters M, Camacho R,
302 Shapiro B, Rambaut A, Vandamme AM: 2005. Recombination is confounding the

- 303 early evolutionary history of HIV-1: subtype G is a circulating recombinant form. *J.*
304 *Virol.* **81**:8543–8551.
- 305 [2] **Alcantara LCJ, Cassol S, Libin P, Deforche K, Pybus OG, Van Ranst M,**
306 **Galvão-Castro B, Vandamme AM, de Oliveira T:** 2009. A standardized frame-
307 work for accurate, high-throughput genotyping of recombinant and non-recombinant
308 viral sequences. *Nucl. Acids Res.* **37**:W634–W642.
- 309 [3] **Althaus CL, Bonhoeffer S:** 2005. Stochastic interplay between mutation and recom-
310 bination during the acquisition of drug resistance mutations in human immunodeficiency
311 virus type 1. *J. Virol.* **79**:13572–13578.
- 312 [4] **de Oliveira T, Deforche K, Cassol S, Salminen M, Paraskevis D, Seebregts C,**
313 **Snoeck J, Janse van Rensburg E, Wensing AMJ, van de Vijver DA, Boucher**
314 **CA, Camacho R, Vandamme AM:** 2005. An automated genotyping system for
315 analysis of HIV-1 and other microbial sequences. *Bioinformatics* **21**:3797–3800.
- 316 [5] **de Oliveira T, Pybus OG, Rambaut A, Salemi M, Cassol S, Ciccozzi M,**
317 **Rezza G, Castelli Gattinara G, D’Arrigo R, Amicosante M, Perrin L, Colizzi**
318 **V, Perno CF, Benghazi Study Group:** 2006. Molecular epidemiology: HIV-1 and
319 HCV sequences from Libyan outbreak. *Nature* **444**:836–837.
- 320 [6] **D’haeseleer P:** 2006. What are DNA sequence motifs? *Nat. Biotechnol.* **24**:423–425.
- 321 [7] **Efron B, Halloran E, Holmes S:** 1996. Bootstrap confidence levels for phylogenetic
322 trees. *Proc. Natl. Acad. Sci. USA* **93**:13429–13434.
- 323 [8] **Felsenstein J:** 1985. Confidence limits on phylogenies: An approach using the boot-
324 strap. *Evolution* **39**:783–791.

- 325 [9] **Gentzsch W**: 2007. Sun grid engine: Towards creating a compute power grid. *In*
326 Proceedings of the 1st International Symposium on Cluster Computing and the Grid
327 (CCGRID 2001), p. 35. IEEE Computer Society, Washington, DC, USA.
- 328 [10] **Holmes EC**: 2008. Evolutionary history and phylogeography of human viruses. *Annu.*
329 *Rev. Microbiol.* **62**:307–328.
- 330 [11] **Jetzt AE, Yu H, Klarmann G, Ron Y, Preston BD, Dougherty JP**: 2000. High
331 rate of recombination throughout the human immunodeficiency virus type 1 genome.
332 *J. Virol.* **74**:1234–1240.
- 333 [12] **Kosakovsky P, Posada D, Gravenor MB, Woelk CH, Frost SDW**: 2006.
334 Gard: a genetic algorithm for recombination detection. *Bioinformatics* **22**:3096–2098.
- 335 [13] **Lemey P, Posada D**: 2009. Introduction to recombination detection. *In* **Lemey P,**
336 **Salemi M, Anne-Mieke V** (eds.), *The Phylogenetic Handbook: a Practical Approach*
337 *to Phylogenetic Analysis and Hypothesis Testing*, 2nd ed., pp. 489–514. Cambridge
338 University Press, Cambridge.
- 339 [14] **Lemey P, Salemi M, Anne-Mieke V**: 2009. *The Phylogenetic Handbook: a Prac-*
340 *tical Approach to Phylogenetic Analysis and Hypothesis Testing*. 2nd ed. Cambridge
341 University Press, Cambridge.
- 342 [15] **Lole KS, Bollinger RC, Paranjape RS, Gadkari D, Kulkarni SS, Novak NG,**
343 **Ingersoll R, Sheppard HW, Ray SC**: 1999. Full-length human immunodeficiency
344 virus type 1 genomes from subtype C-infected seroconverters in India, with evidence of
345 intersubtype recombination. *J. Virol.* **73**:152–160.
- 346 [16] **Martin DP, Biagini P, Lefevre P, Golden M, Roumagnac P, Varsani A**: 2011.
347 Recombination in eukaryotic single stranded dna viruses. *Viruses* **3**:1699–1738.

- 348 [17] **Martin DP, Lemey P, Lott M, Moulton V, Posada D, Lefevre P**: 2010.
349 RDP3: a flexible and fast computer program for analyzing recombination. *Bioinformat-*
350 *ics* **19**:2462–2463.
- 351 [18] **Minh BQ, Vinh LS, von Haeseler A, Schmidt HA**: 2005. pIQPNNI – parallel
352 reconstruction of large maximum likelihood phylogenies. *Bioinformatics* **21**:3794–3796.
- 353 [19] **Paraskevis D, Pybus O, Magiorkinis G, Hatzakis A, Wensing AMJ, van de**
354 **Vijver DA, Albert J, Angarano G, Asjo B, Balotta C, Boeri E, Cama-**
355 **cho R, Chaix ML, Coughlan S, Costagliola D, De Luca A, de Mendoza**
356 **C, Derdelinckx I, Grossman Z, Hamouda O, Hoepelman AIM, Horban A,**
357 **Korn K, Kuecherer C, Leitner T, Loveday C, Macrae E, Maljkovic I, Meyer**
358 **L, Nielsen C, Op de Coul ELM, Ormaasen V, Perrin L, Puchhammer-Stockl**
359 **E, Ruiz L, Salminen M, Schmit JC, Schuurman R, Soriano V, Stanczak JJ**:
360 2009. Tracing the HIV-1 subtype B mobility in Europe: a phylogeographic approach.
361 *Retrovirol.* **6**:49.
- 362 [20] **Pybus OG, Suchard MA, Lemey P, Bernardin FJ, Rambaut A, Crawford**
363 **FW, Gray RR, Arinaminpathy N, Stramer SL, Busch MP, Delwart EL**: 2012.
364 Unifying the spatial epidemiology and molecular evolution of emerging epidemics. *Proc.*
365 *Natl. Acad. Sci. USA* **109**:in press.
- 366 [21] **Rambaut A, Grassly NC**: 1997. Seq-Gen: An application for the Monte Carlo
367 simulation of DNA sequence evolution along phylogenetic trees. *Comput. Appl. Biosci.*
368 **13**:235–238.
- 369 [22] **Salminen M, Martin D**: 2009. Detecting and characterizing individual recombination
370 events. *In* **Lemey P, Salemi M, Anne-Mieke V** (eds.), *The Phylogenetic Handbook*:

- 371 a Practical Approach to Phylogenetic Analysis and Hypothesis Testing, 2nd ed., pp.
372 515–544. Cambridge University Press, Cambridge.
- 373 [23] **Salminen MO, Carr JK, Burke DS, McCutchan FE**: 1995. Identification of
374 breakpoints in intergenotypic recombinants of HIV type 1 by bootscanning. *AIDS Res.*
375 *Hum. Retroviruses* **11**:1423–1425.
- 376 [24] **Sanderson MJ, Shaffer HB**: 2002. Troubleshooting molecular phylogenetic analyses.
377 *Annu. Rev. Ecol. Syst.* **33**:49–72.
- 378 [25] **Schmidt HA, Strimmer K, Vingron M, von Haeseler A**: 2002. TREE-PUZZLE:
379 Maximum likelihood phylogenetic analysis using quartets and parallel computing. *Bioin-*
380 *formatics* **18**:502–504.
- 381 [26] **Schmidt HA, von Haeseler A**: 2009. Phylogenetic inference using maximum likeli-
382 hood methods. *In* **Lemey P, Salemi M, Anne-Mieke V** (eds.), *The Phylogenetic*
383 *Handbook: a Practical Approach to Phylogenetic Analysis and Hypothesis Testing*, 2nd
384 ed., pp. 181–209. Cambridge University Press, Cambridge.
- 385 [27] **Simon-Loriere E, Holmes EC**: 2011. Why do RNA viruses recombine? *Nat. Rev.*
386 *Microbiol.* **9**:617–626.
- 387 [28] **Strimmer K, von Haeseler A**: 1996. Quartet puzzling: A quartet maximum-
388 likelihood method for reconstructing tree topologies. *Mol. Biol. Evol.* **13**:964–969.
- 389 [29] **Strimmer K, von Haeseler A**: 1997. Likelihood-mapping: A simple method to
390 visualize phylogenetic content of a sequence alignment. *Proc. Natl. Acad. Sci. USA*
391 **94**:6815–6819.
- 392 [30] **Swofford DL, Olsen GJ, Waddell PJ, Hillis DM**: 1996. Phylogeny reconstruction.

- 393 *In* **Hillis DM, Moritz C, Mable BK** (eds.), *Molecular Systematics*, 2nd ed., pp. 407–
394 514. Sinauer Associates, Sunderland, Massachusetts.
- 395 [31] **Thain D, Tannenbaum T, Livny M**: 2005. Distributed computing in practice: the
396 Condor experience. *Concurr. Comput.-Pract. Exp.* **17**:323–356.
- 397 [32] **Tschager T, Schmidt HA**: 2012. DAGwoman: enabling DAGman-like workflows on
398 non-Condor platforms. *In* *Proceedings of the 1st ACM SIGMOD Workshop on Scalable
399 Workflow Execution Engines and Technologies (SWEET 2012)*. ACM, New York, NY,
400 USA.

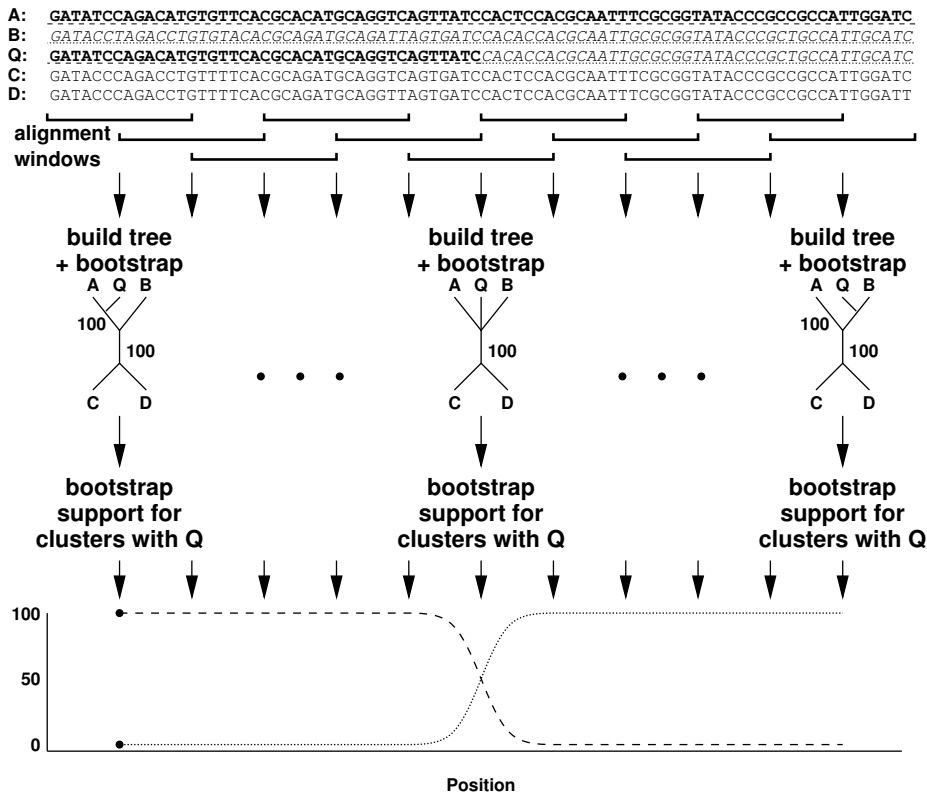


Figure 1 – Principle of bootscanning analysis.

Four reference groups $\{A\}$, $\{B\}$, $\{C\}$ and $\{D\}$ plus a query group $\{Q\}$ serve as input. Divide the alignment into overlapping windows. For each window bootstrap tree reconstruction is performed and the number of $\{Q, A\}$ and $\{Q, B\}$ branches in the bootstrap trees are evaluated for each window. The resulting bootscan plot at the bottom shows the case that Q is a recombinant containing the first half sequence of A (dashed curve or underline) and the second half of B (dotted curve or underline).

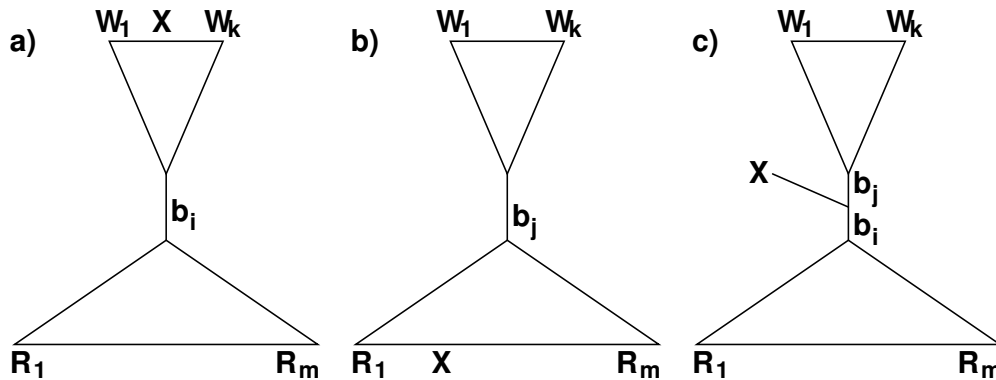


Figure 2 – Ignoring sequences in the analysis.

There are 3 scenarios when determining the support of $\{W_1 \dots W_k\}$ in reconstructed bootstrap trees excluding a sequence X . The triangles depict subtrees containing the sequences at their leaves. (a) If X is located within (but not basal to) the subtree of $\{W_1 \dots W_k\}$ then b_i is used as the bootstrap support. (b) If X is not located within the subtree of $\{W_1 \dots W_k\}$ but among (but not basal to) the remaining sequences $\{R_1 \dots R_m\}$ then b_j gives the bootstrap support. (c) In the special case that X is located between the subtrees of $\{W_1 \dots W_k\}$ and $\{R_1 \dots R_m\}$ then b_i and b_j exist at the same time in a tree. In all cases $\max(b_i, b_j)$ is used as the bootstrap support for $\{W_1 \dots W_k\}$.

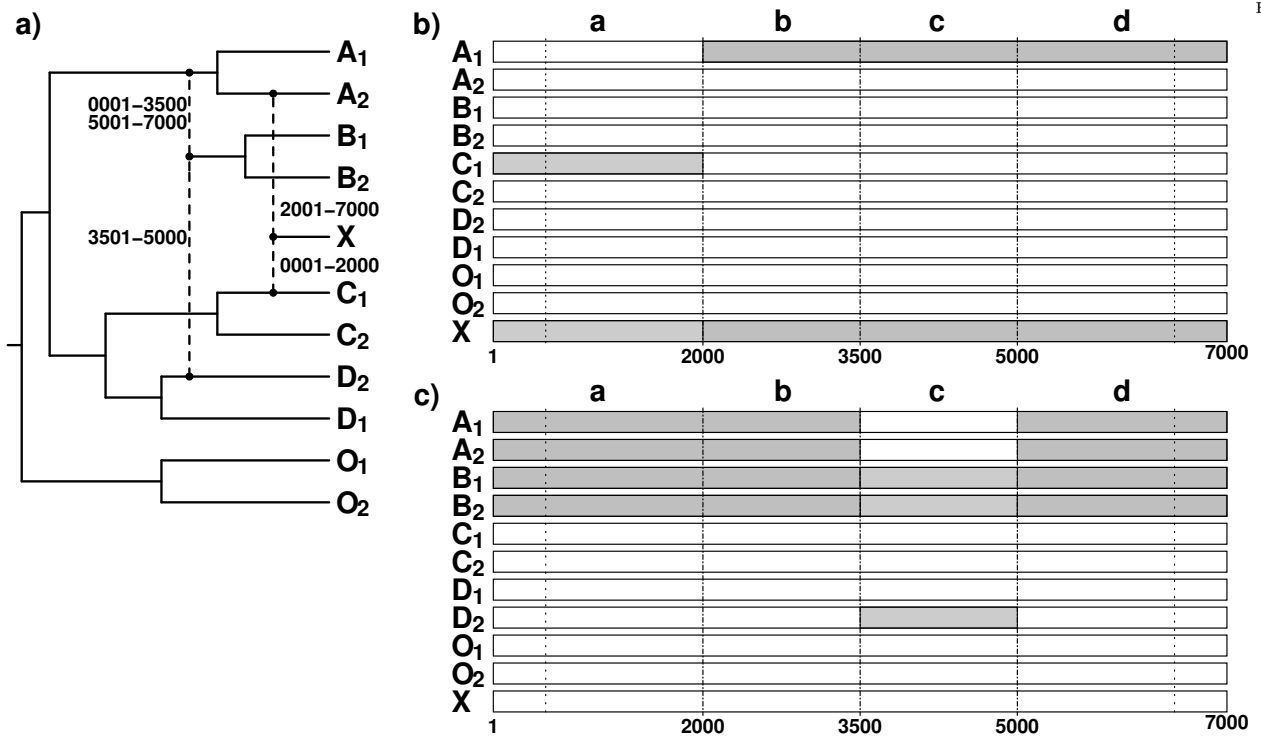


Figure 3 – Simulating an overlapping recombination scenario.

(a) The recombination graph shows the two overlapping recombinations, where the dashed lines depict the different genomic sources of the recombinant genomes. X arises from a recombination of an ancestor of $C2$ with an ancestor of $A1$, while $\{B1, B2\}$ arise from a recombination of the ancestor of $\{A1, A2\}$ with $D2$. The recombinations are overlapping because X and $\{B1, B2\}$ both share a common history with sequences from the reference group $\{A1, A2\}$ in the same regions **b** and **d**. The relationships are reflected accordingly by the shaded areas in the sequence alignment: (b) X and $C1$ share a common history in region **a**, X and $A1$ share a common history in regions **b,c,d**. (c) $\{B1, B2\}$ and $D2$ share a common history in region **c**, otherwise $\{B1, B2\}$ and $\{A1, A2\}$ share a common history.

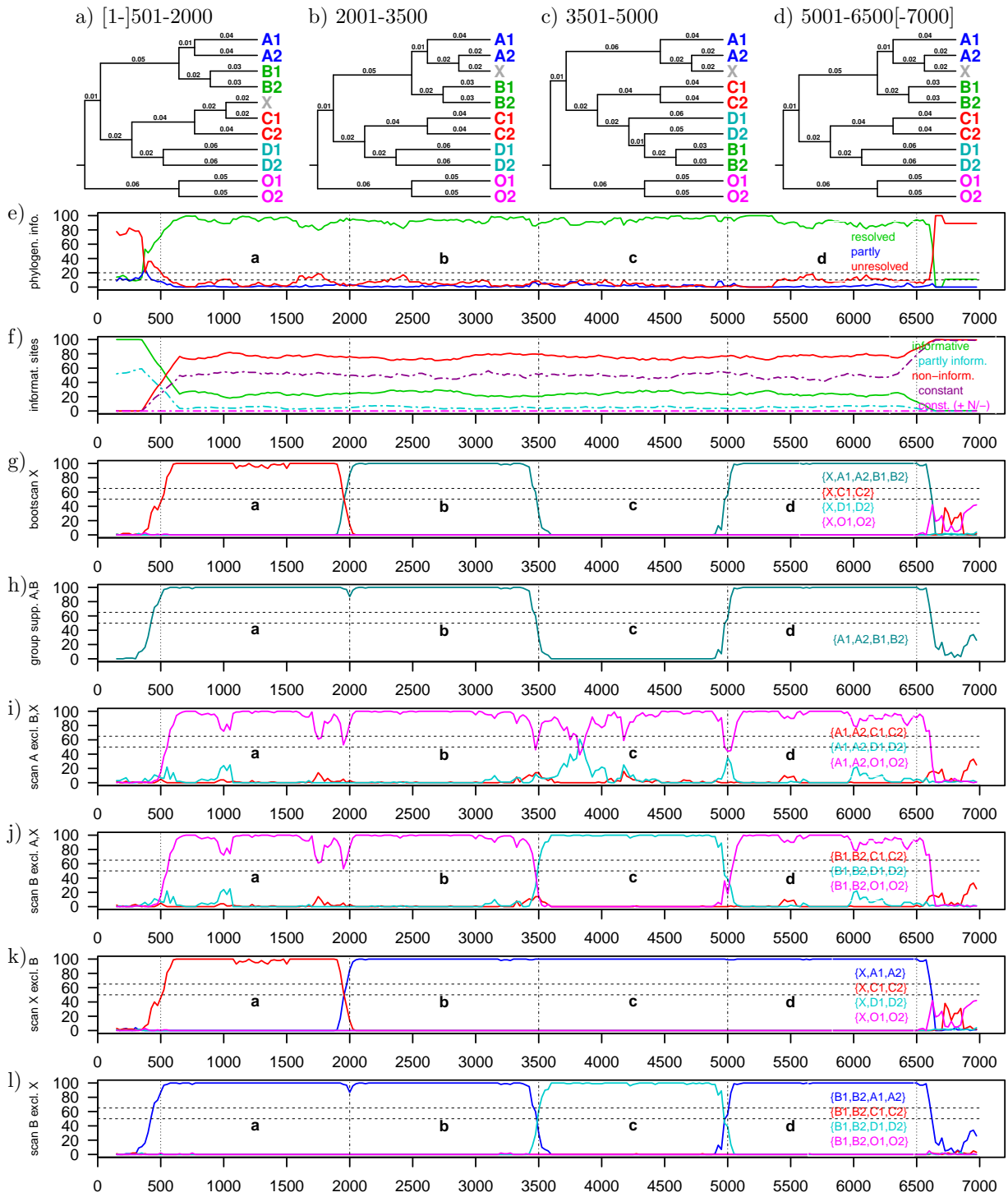


Figure 4 – Analysis of an example with overlapping recombinations.

(a)-(d) evolutionary histories for the genomic regions 1-2000, 2001-3500, 3501-5000 and 5001-7000 (regions **a-d**), where in regions 1-500 and 6501-7000 the branch lengths have been extended and reduced by factors of 50, respectively. (e) Visualization of phylogenetic signal along the alignment by likelihood mapping along the alignment. (f) Visualization of the content of informative sites along the alignment. (g) ML bootscan plot for the recombinant $\{X\}$. (h) ML bootstrap support for the erroneously grouped sequences of $\{A1, A2, B1, B2\}$. (i) ML bootscan plot for $\{A1, A2\}$ only, excluding $\{X\}$ and $\{B1, B2\}$. (j) ML bootscan plot for $\{B1, B2\}$ only, excluding $\{X\}$ and $\{A1, A2\}$. (k) ML bootscan plot for $\{X\}$ when excluding $\{B1, B2\}$. (l) ML bootscan plot for recombinant group $\{B1, B2\}$ excluding sequence $\{X\}$. For more details see text. The vertical lines mark the recombination break points and the border to the regions of increased or decreased variability at the ends.

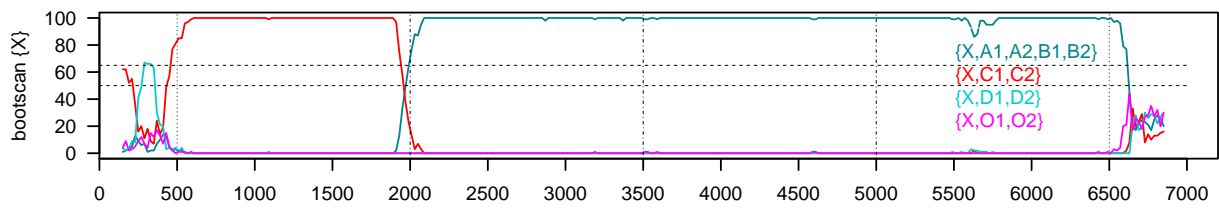


Fig. 5

Figure 5 – Bootscan with groups condensed to sequences.

Diagram from results of SimPlot which condenses groups to consensus sequences plotted the same way and using the same window size as in Fig. 4 for comparability.